Available online at www.sciencedirect.com
SCIENCE DIRECT®
Engineering Structures 25 (2003) 951–964
ENGINEERING STRUCTURES
www.elsevier.com/locate/engstruct

Optimal design of reinforced concrete T-sections in bending

C.C. Ferreira [a,*], M.H.F.M. Barros [a], A.F.M. Barros [b]

[a] *Department of Civil Engineering, Faculty of Sciences and Technology, University of Coimbra, Polo II, 3030 Coimbra, Portugal*
[b] *IDMEC/Instituto Superior Técnico, Av. Rovisco Pais, 1000 Lisbon, Portugal*

Received 9 August 2002; received in revised form 3 February 2003; accepted 4 February 2003

Abstract

The optimisation of the steel area and the steel localisation in a T-beam under bending is carried out in the present work. The expressions giving the equilibrium of a singly or doubly reinforced T-section in the different stages defined by the non-linear behaviour of steel and concrete are derived ones. The ultimate material behaviour is defined according to the design codes such as EC2 and Model Code 1990. The purpose of this work is to obtain the analytical optimal design of the reinforcement of a T-section, in terms of the ultimate design. In the last section the expressions developed are applied to examples and design abacus are delivered. A comparison is made with current practice method as indicated in CEB.

Keywords: Reinforced concrete; Double reinforcement; T-sections; Optimisation of the reinforcement; Design abacus

1. Introduction

Methods based on optimality criteria can be applied to reinforced concrete structures in order to obtain the minimum cost design. The costs to be minimised are generally divided into those of concrete, steel and formwork. This means that they include one or more of the following variables: the geometry of the section of beams and columns; the area and topology of the steel reinforcement. Methods based on this kind of analysis are found in references [1–5]. Nevertheless, these optimisations consider a linear elastic analysis of the global structure. This type of linear analysis is relevant for the serviceability limit state design and it is important for the definitive dimensions of the sections. In terms of the ultimate limit design of concrete structures, this analysis is not correct due to the non-linear behaviour of reinforced concrete.

Considering design variables such as section dimensions, steel area and topology at the same time, the non-linear optimisation of reinforced concrete structures is a very complex and yet to be solved problem. Optimising the dimensions of the sections within serviceability conditions and then optimising the steel area and location in the ultimate limit design within a non-linear analysis, appears to be a good solution. As a matter of fact, the design codes [6,7] suggest that non-linear analysis can be replaced by linear analysis with redistribution of the moments and the design of the reinforced concrete members being made for the critical sections, where the bending moment and shear attain their maximum value. The optimisation of the reinforcement in a section is developed within this context.

The optimal design of the critical sections is known only for rectangular sections. For other geometries, research has been made in terms of the biaxial interaction diagrams [8–10]. These diagrams attempt to make an optimisation by a trial and error procedure. The importance of the development of the optimal design of T-sections is due to the fact that it is currently a frequently used section in common structures. Another relevant aspect is that the methodology used can be extended to other sections and included in the computer codes with minimum programming.

The design variables considered in the optimisation of the reinforced beam with a T-section are the steel area and the steel localisation, either in the tension or in the compression zones. The equilibrium equations of a reinforced concrete T-section under Limit State Design,

* Corresponding author. Tel.: +351-239-797-100; fax: +351-239-797-123.
E-mail address: carla@dec.uc.pt (C.C. Ferreira).

0141-0296/03/$ - see front matter © 2003 Elsevier Science Ltd. All rights reserved.
doi:10.1016/S0141-0296(03)00039-7

as defined by the non-linear behaviour of the concrete and the steel, are developed for this purpose.

The examples presented consist of the optimisation of the reinforcement of a T-section for different geometric definitions. The results are compared with the design obtained in current practice methods such as the one indicated in CEB [11].

2. Ultimate design of reinforced concrete section under bending

2.1. Geometry of the T-section

The T-section geometry of the reinforced concrete structure is defined by the following parameters, as shown in Fig. 1: lower steel area in the tensile zone, A_s; upper steel area near the compression zone, A'_s; the flange depth, h_f ; the effective flange width, b; the web width, b_w; the distance from the centroid of the reinforcement to opposite face of the section, d; the concrete cover, a.

In the present work, the design variable in the optimisation process is the ratio A'_s/A_s, since, for a given total area of reinforcement $A_s + A'_s$, the objective function is to maximise the bending moment. As a matter of fact, for a given bending moment, the global area of reinforcement is only a function of the ratio A'_s/A_s, which, for this reason, is the only design variable in terms of the limit state design of the section. The cover of steel is not considered as a design variable because it is fixed, in each case, by durability conditions. The equations are developed as a function of the non-dimensional variables a/d, b_w/b and h_f/d.

2.2. Constitutive laws

The ultimate design of reinforced concrete sections under bending moment is defined in terms of non-linear constitutive laws of the concrete and the steel. The stress–strain equation for concrete used in the design codes is defined by a parabola followed by a constant

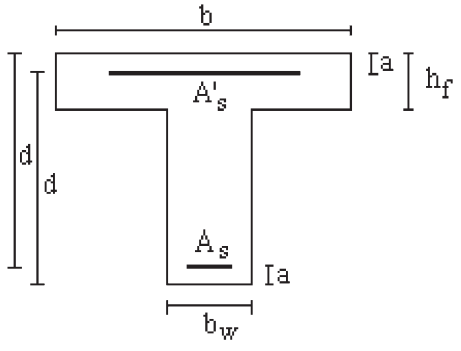

Fig. 1. Geometry of the doubly reinforced T-section.

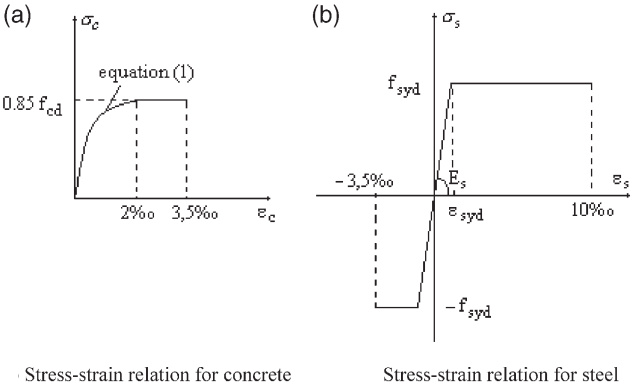

Fig. 2. Design stress–strain diagrams.

value, usually called parabola–rectangle law and represented in Fig. 2(a). The maximum stress is equal to $0.85f_{cd}$, where f_{cd} is the design strength of the concrete under compression. It is considered that concrete in ultimate design does not stand for tensile stresses. The equation for the parabola is function of the concrete deformation ε_c, as follows:

$$\sigma_c = 850f_{cd}(\varepsilon_c - 250\varepsilon_c^2) \text{for } \varepsilon_c \leq 0.002 \quad (1)$$

The design stress–strain law for steel is elastic-perfectly plastic with a maximum value f_{syd} , which is the design value for the strength of steel, equal in tension and compression. This law is represented in Fig. 2(b). The steel has initial elastic behaviour with the elasticity modulus E_s. The elastic domain is valid until the maximum design stress f_{syd} is reached, corresponding to the maximum elastic strain ε_{syd}.

2.3. Rupture conditions

The limit design means that rupture is considered when the strains in the section reach maximum values, which are different for concrete and steel. Concrete is considered to crush at $\varepsilon_c = 0.35\%$. The steel rupture under compression is limited to 0.35% due to the crush of the concrete, and to 1% under tension. These conditions are represented in Fig. 3, where the section before deformation is represented by the vertical line and after

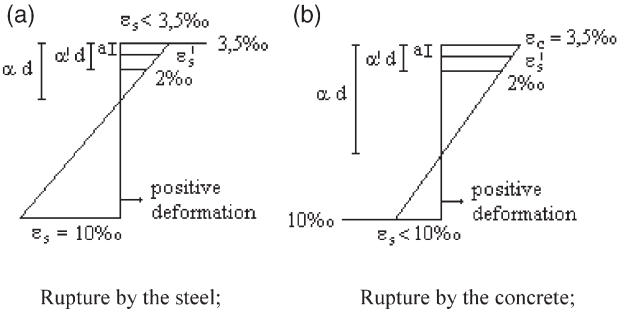

Fig. 3. Rupture of the section.

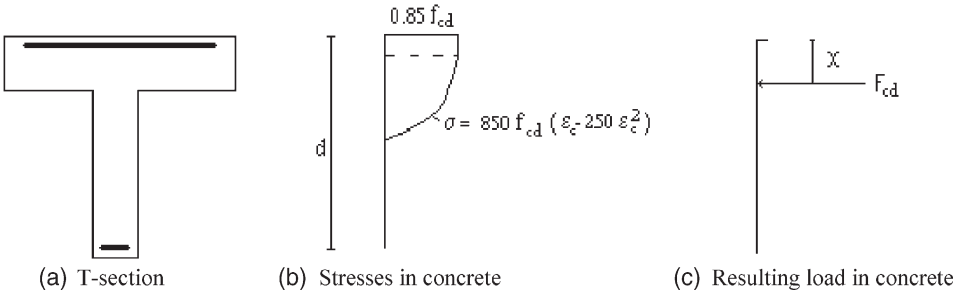

Fig. 4. (a) T-section; (b) stresses in concrete; (c) resulting load in concrete.

Table 1
Values of m_1

	$0 < \varepsilon'_s < \frac{f_{syd}}{E_s}$	$\varepsilon'_s \geq \frac{f_{syd}}{E_s}$
m_1	$\frac{E_s \varepsilon'_s}{f_{syd}}$	1

deformation by the inclined line. In both ruptures, by the steel [Fig. 3(a) and by the concrete [Fig. 3(b)], the neutral axis is located at the distance αd from the upper zone, and α is given by:

$$\frac{\varepsilon_c}{\varepsilon_c - \varepsilon_s} \tag{2}$$

The parabola–rectangle transition is located at the distance $\alpha' d$ from the upper zone and corresponds to the concrete strain $\varepsilon_c = 0.2\%$.

In the Fig. 3, the strain in upper reinforcement, ε'_s, is also indicated, and is computed by:

$$\varepsilon'_s = (\varepsilon_c - \varepsilon_s)\left(\alpha - \frac{a}{d}\right) \tag{3}$$

The stresses in the concrete under compression, corresponding to the strains represented in Fig. 3, are indicated in Fig. 4(b). The stresses upon the steel in the upper reinforcement of the compression zone are termed m_1 and are detailed in Table 1. The stresses upon the steel in the lower reinforcement of the tensile zone, are termed m_2 and are presented in Table 2.

Table 2
Values of m_2

	$0 < -\varepsilon_s \leq \frac{f_{syd}}{E_s}$	$\frac{f_{syd}}{E_s} < -\varepsilon_s < 1\%$
m_2	$\frac{E_s \varepsilon_s}{f_{syd}}$	-1

2.4. Resulting load in the concrete

The resulting load in concrete, F_{cd}, is obtained by the integration of the stresses in the concrete, that is the second degree Eq. (1), called parabola, and the constant value, called rectangle. These stresses may be applied either in the flange or in the web. Considering the variation of neutral axis αd and the flange depth h_f, the rupture conditions are also variable. The consideration of all possibilities originates the several cases described in Fig. 5.

The value of the resulting load, in each case i, is denoted by F^i_{cd} and the distance to the upper edge of the section by X^i. The load in concrete can be written in non-dimensional form, $F^i_{cd_{red}}$, defined by the following expression:

$$F^i_{cd_{red}} = \frac{F^i_{cd}}{f_{cd} b\, d}. \tag{4}$$

The value of all $F^i_{cd_{red}}$ and X^i are given in Appendix A.

There are VIII cases to be considered. In cases I and II rupture occurs in steel and concrete which has a stress

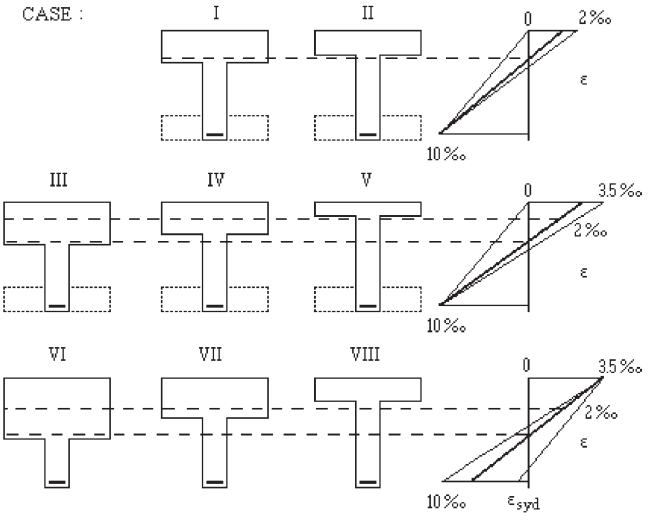

Fig. 5. Different cases considered in the computation of the resulting load.

ε_c lower than 0.2% (see Fig. 5). In cases III–V rupture is also in the steel but concrete strain ε_c is larger than 0.2%. In cases VI–VIII rupture is in concrete with strain equal to 0.35%. The cases can also be grouped in terms of the flange depth. Cases I, III, and VI can be called the cases for high flange depth. The neutral axis is in the flange and the section is equivalent to a rectangular section in terms of the rupture condition. Cases II, V and VIII can be related by the fact that the flange depth is small. Cases IV and VII are intermediate to the others and correspond to medium depth flange.

2.5. Equilibrium equations in the section

The equilibrium equations of all the loads acting on the section, when zero axial force is applied and a bending moment is imposed, establishes the expressions (5) and (8). The first one is:

$$F^i_{cd_{red}} + \frac{A'_s}{A_s} w\, m_1 + w\, m_2 = 0 \tag{5}$$

where m_1 and m_2 were previously defined (Tables 1 and 2), w is the percentile of the lower reinforcement, calculated, through:

$$w = \frac{A_s f_{syd}}{bd\, f_{cd}}. \tag{6}$$

Considering a bending moment M_{sd} applied to the section and the reduced bending moment as:

$$\mu = \frac{M_{sd}}{d^2 b\, f_{cd}}, \tag{7}$$

the second equilibrium condition is written as:

$$F^i_{cd_{red}}\left(1 - \frac{X^i}{d}\right) + \frac{A'_s}{A_s} w \left(1 - \frac{a}{d}\right) m_1 - \mu = 0 \tag{8}$$

It must be remarked that there are as many equations as the number of cases denoted in Fig. 5.

3. Minimum area of the reinforcement

3.1. Objective function

The optimisation problems concern the achievement of the best solution for a given objective function satisfying certain conditions.

Currently, the design is made for the most stressed section that delimits the cross section dimensions and the amount of steel. Optimisation of the steel area, in a predefined cross section, is similar to computing the minimum rate of steel. In practice, the computation of different rates with different locations, using design tables, approaches the optimal solution by trial. For the designer, the purpose is to establish the expression giving the maximum resistant bending moment, function of the area and location of the reinforcement with the relation A'_s/A_s.

In the present problem the system of Eqs (5) and (8) are the equilibrium equations of the section. Substituting into these expressions the definitions of $F^i_{cd_{red}}$, X^i, m_1 and m_2, they become perfectly defined in terms of the variables $\alpha, \frac{A'_s}{A_s}, \frac{h_f}{d}, \frac{a}{d}, \frac{b}{b_w}, \frac{f_{syd}}{f_{cd}}$ and can be written respectively in the form:

$$w = g\left(\alpha, \frac{A'_s}{A_s}, \frac{h_f}{d}, \frac{a}{d}, \frac{b}{b_w}, \frac{f_{syd}}{f_{cd}}\right) \tag{9}$$

$$\mu = f\left(\alpha, \frac{A'_s}{A_s}, \frac{h_f}{d}, \frac{a}{d}, \frac{b}{b_w}, \frac{f_{syd}}{f_{cd}}\right) \tag{10}$$

In practical terms, the purpose is to maximise the bending moment μ, Eq. (10), with the constraint defined by Eq. (9).

3.2. Design variables

The variables defining the position of the steel in the section are used in the optimisation process in the present work. This is the ratio of steel areas A'_s/A_s. The total area of reinforcement is given by the sum A'_s and A_s and is considered in the constrain Eq. (9). In non-dimensional terms, it is defined by w_t, that is the percentile reinforcement given by:

$$w_t = \frac{A_s + A'_s f_{syd}}{bd\ f_{cd}} = \left(1 + \frac{A'_s}{A_s}\right) w \tag{11}$$

This total reinforcement can also be written in function of all variables, by using Eq. (9):

$$w_t = \left(1 + \frac{A'_s}{A_s}\right) g\left(\alpha, \frac{A'_s}{A_s}, \frac{h_f}{d}, \frac{a}{d}, \frac{b}{b_w}, \frac{f_{syd}}{f_{cd}}\right) \tag{12}$$

The arguments $\frac{a}{d}$ and $\frac{f_{syd}}{f_{cd}}$ in Eqs (9) and (10) are not considered design variables since $\frac{a}{d}$ is usually imposed by durability and other construction requirements. The strength ratio $\frac{f_{syd}}{f_{cd}}$ is a known value after the choice of the materials. The geometry parameters $\frac{h_f}{d}$ and $\frac{b}{b_w}$ can be used as design variables in the case of shape optimisation of the section.

After eliminating the described constant parameters, Eqs (12) and (10) become respectively:

$$w_t = \left(1 + \frac{A'_s}{A_s}\right) g\left(\alpha, \frac{A'_s}{A_s}\right) \tag{13}$$

$$\mu = f\left(\alpha, \frac{A_s'}{A_s}\right) \tag{14}$$

Choosing μ as the objective function and w_t as an imposed variable, Eq. (13) can be solved in terms of α, that is:

$$\alpha = h\left(\frac{A_s'}{A_s}\right) \tag{15}$$

The value α is turned into the objective function, Eq. (14), that becomes:

$$\mu = f\left(h\left(\frac{A_s'}{A_s}\right), \frac{A_s'}{A_s}\right) \tag{16}$$

This equation shows that, in the present work, there is only one design variable, A_s'/A_s, but the objective function is defined as a piecewise function, giving as many different expressions as the cases of Fig. 5. As the constant characteristics of the arguments are accepted, $\frac{a}{d}$, $\frac{b}{b_w}$, $\frac{h_f}{d}$ and $\frac{f_{syd}}{f_{cd}}$, the analytical optimal solution is always written in terms of those arguments.

3.3. Optimal neutral axis depth

In the present work, the choice of the formula for the mathematical optimisation problem does not allow the calculus of the sensibilities due to the characteristic discontinuity of the objective function. The optimal solution is obtained by considering an increment of the design variable A'_s/A_s, that is dA'_s/A_s, giving the following value of the objective function:

$$\mu^* = f\left(h\left(\frac{A_s'}{A_s} + \frac{dA_s'}{A_s}\right), \frac{A_s'}{A_s} + \frac{dA_s'}{A_s}\right) \tag{17}$$

The function has a stationary value since a maximum or a minimum point exists and Eqs (16) and (17) should be equal when dA'_s/A_s approaches zero, such as:

$$f\left(\alpha, \frac{A_s'}{A_s}\right) = \lim_{\frac{dA_s'}{A_s} \to 0} f\left(h\left(\frac{A_s'}{A_s} + \frac{dA_s'}{A_s}\right), \frac{A_s'}{A_s} + \frac{dA_s'}{A_s}\right) \tag{18}$$

This equation is solved for each of the cases in Fig. 5, giving for high flange depth (cases I, III and VI) the optimal value of neutral axis depth, α^* , given by:

$$\alpha^* = \frac{119}{198}\left(1 + \frac{a}{d}\right) \tag{19}$$

With this optimal value, the minimum flange depth available for these cases I, III and VI can be established by:

$$\frac{h_f}{d} \geq \alpha^* = \frac{119}{198}\left(1 + \frac{a}{d}\right) \tag{20}$$

The optimal solution obtained from Eq. (18), for the cases of small flange depth (cases II, V and VIII), is the same value α^* of expression (19). The limit value of the flange depth, $\frac{h_f}{d}$, is obtained by imposing the limits of these cases, as shown in Fig. 6, and becomes:

$$\frac{h_f}{d} \leq \frac{17}{66}\left(1 + \frac{a}{d}\right) \tag{21}$$

For the intermediate values of the flange depth, corresponding to cases IV and VII, the optimal solution can not be obtained analytically through Eq. (18) in function of the parameters. The computation of the optimal neutral axis depth using Eq. (18) is possible only when discrete values of the different parameters are imposed. For this reason an approximate solution for cases IV and VII is proposed in section 3.6.

3.4. Ductility limitation

The position of neutral axis affects the deformation of the steel, that can be in the elastic or in the plastic domain. In the design of reinforced concrete, it is important to guarantee a certain ductility. The condition for the plasticity of the lower steel A_s, defined by a limit value of α, termed α_p, depends on the designed yield strain ϵ_{syd}, that varies for each class of steel. This limit for the plastic zone of the steel α_p is the following:

$$\alpha_p = \frac{7}{7 + 2000\varepsilon_{syd}}. \tag{22}$$

The plastic limits α_p Eq. (22), defined for three classes of steel, namely S235, S400 and S500, are represented in Fig. 7. The optimal value $\alpha*$ Eq. (19), is also represented in Fig. 7. Since the condition of applicability of $\alpha*$ is the yielding of steel A_s, as imposed in cases I–VIII, the corresponding equation is only valid when it satisfies the following inequality:

$$\alpha^* \leq \alpha_p \tag{23}$$

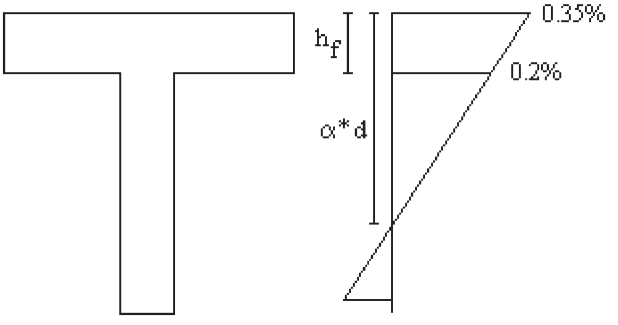

Fig. 6. Limit zone for $\frac{h_f}{d}$ in case VIII.

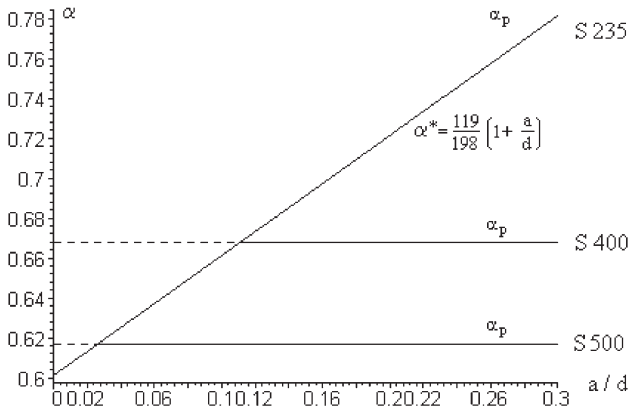

Fig. 7. Optimal neutral axis depth: α^* or α_p.

As a result, for a given a/d, the optimum value for α is either α^* or α_p whichever the smaller value might be.

3.5. Optimal solution and design

The optimal solution of the design variable $(A'_s/A_s)^*$ is obtained by solving Eq. (15) in terms of A'_s/A_s and substituting in it α^* or α_p, that is:

$$\left(\frac{A'_s}{A_s}\right)^* = h^{-1}(\alpha^* \text{ or } \alpha_p) \tag{24}$$

For a small bending moment there is no reinforcement in the compression zone, meaning that $A'_s = 0$. The limit value of the bending moment can be termed as economic moment μ_e and is obtained by replacing α^* or α_p and $A'_s/A_s = 0$ into Eq. (14), which becomes:

$$\mu_e = f(\alpha^* \text{ or } \alpha_p) \tag{25}$$

This value is relevant for the practical design of reinforced concrete sections as well as for the optimal area of reinforcement ω_t^*. The optimal area of reinforcement is obtained by replacing the values α^* and $(A'_s/A_s)^*$ in Eq. (13), that is:

$$\omega_t^* = \left(1 + \left(\frac{A'_s}{A_s}\right)^*\right) g\left(\alpha^* \text{ or } \alpha_p, \left(\frac{A'_s}{A_s}\right)^*\right) \tag{26}$$

If only the area A_s is considered, the optimum percentile lower reinforcement ω^*, Eq. (9), becomes:

$$\omega^* = g\left(\alpha^* \text{ or } \alpha_p, \left(\frac{A'_s}{A_s}\right)^*\right) \tag{27}$$

3.6. Approximate solution in cases IV and VII

For the cases IV and VII the optimal solution is only obtained if values for h_f/d and b_w/b are prescribed, preventing a generally analytical solution. In practical terms, it may be relevant to have design expressions since they have small errors. For this reason, the approximate value considered in cases IV and VII is α^*, Eq. (19), satisfying the following condition:

$$\alpha_{apr} = \frac{119}{198}\left(1 + \frac{a}{d}\right) \leq \alpha_p \tag{28}$$

In order to determine the error introduced by the approximate neutral axis depth α_{apr} in the optimal design of the section, the computation of optimal neutral axis depth α^* was reached, according to section 3.3, for a representative number of prescribed values of h_f/d and b_w/b and a/d. Replacing these optimal α^* successively in expressions (14) and (13), the corresponding percentile of reinforcement w_{real} was found. The values of the percentile of reinforcement w_{apro}, obtained when α_{apr} is considered in expressions (14) and (13), were also computed. The error introduced in the optimal design was evaluated by the following expression:

$$\frac{w_{apro} - w_{real}}{w_{real}} \times 100 \tag{29}$$

Table 3 gives the values of this definition of error for $b/b_w = 2, 3, 4, 5, 6, 7, 8, 9, 10$, with $a/d = 0.05$ and h_f/d varying from 0.28 to 0.37.

Table 4 exemplifies the errors that can be obtained by the variation of parameter a/d. In Table 4, the values of expression (23) are plotted for $a/d = 0.04, 0.05, 0.06, 0.07, 0.08, 0.09, 0.1$, with $b/b_w = 4$ and h_f/d varying from 0.27 to 0.41. The blank cells in Tables 3 and 4 correspond to the optimal value given by α_p.

Other calculations, similar to the ones related above were made, namely fixing the parameter b/b_w and computing the error with variable h_f/d and a/d, as made in Table 4. The results are missed out but they are always less than 0.14%. This is the reason why expression (22) was considered a good approximation to the optimal solution.

4. Examples

The optimal neutral axis depth and the corresponding expressions of the design, obtained according to section 3.5, was found for a general T-section. The expressions obtained in these computations are developed in Appendix B and they are presented in Table 5, with their respective limitations.

4.1. Abacus for optimal design

The developed expressions are applied in a T-section for $a/d = 0.1$ with variable geometric definitions of b/b_w:b/b_w equal 1/10, 1/8, 1/6, 1/4 and 1/2. The considered steel classes are S400 or S500. The values of the economic reduced bending moment μ_e are plotted in Fig. 8. Fig. 8 emphasises the limits of expressions (6a), (7a)

Table 3
Error for different values of h_f/d and b/b_w

$b/b_w h_f/d$	2	3	4	5	6	7	8	9	10
0.28	0.000001	0.000003	0.000005	0.000007	0.000009	0.000011	0.000013	0.000015	0.000017
0.29	0.000021	0.000055	0.000089	0.000123	0.000156	0.000189	0.000221	0.000225	0.000280
0.30	0.000110	0.000278	0.000449	0.000616	0.000775	0.000927	0.001072	0.001210	0.001341
0.31	0.000346	0.000865	0.001385	0.001881	0.002347	0.002786	0.003198	0.003585	0.003950
0.32	0.000832	0.002059	0.003265	0.004396	0.005445	0.006416	0.007317	0.008155	0.008937
0.33	0.001689	0.004133	0.006496	0.008675	0.010668	0.012492	0.014165	0.015707	0.017133
0.34	0.003041	0.007374	0.011489	0.015228	0.018604	0.021660	0.024439	0.026977	0.029309
0.35	0.005020	0.012056	0.018629	0.024521	0.029782	0.034498	0.038751	0.042609	0.046129
0.36	0.007747	0.018428	0.028256	0.036956	0.044645	0.051479	0.057597	—	—
0.37	0.011325	0.026694	0.040635	0.052836	0.063520	—	—	—	—
0.38	0.015834	0.036997	0.055939	0.072348	—				
0.39	0.021322	0.049409	0.074241	—	—				
0.40	0.027800	0.063917	0.095489	—	—				
0.41	0.035235	0.080418	—	—	—				

Table 4
Error for different values of h_f/d and a/d

$a/d h_f/d$	0.04	0.05	0.06	0.07	0.08	0.09	0.10
0.27	0.000002	0.000000	0.000000	—	—	—	—
0.28	0.000056	0.000029	0.000014	0.000010	0.000000	0.000000	-0.000000
0.29	0.000335	0.000226	0.000146	0.000089	0.000051	0.000026	0.000012
0.30	0.001121	0.000846	0.000624	0.000449	0.000313	0.000211	0.000135
0.31	0.002770	0.002230	0.001771	0.001385	0.001065	0.000802	0.000591
0.32	0.005680	0.004768	0.003966	0.003265	0.002589	0.002139	0.001697
0.33	0.010255	0.008868	0.007618	0.006496	0.005497	0.004612	0.003835
0.34	0.016752	0.014923	0.013130	0.011488	0.009995	0.008641	0.007421
0.35	0.025870	0.023285	0.020873	0.018629	0.016552	0.014636	0.012876
0.36	0.037498	0.034241	0.031160	0.028256	0.025529	0.022975	0.020594
0.37	0.051922	0.047990	0.044225	0.040634	0.037220	0.033983	—
0.38	0.069199	0.064629	0.060207	0.055940	0.051836	—	—
0.39	0.089266	0.084143	0.079130	0.074241	0.069488	—	—
0.40	0.111929	0.106387	0.100899	0.095488	—	—	—
0.41	0.136864	0.131085	0.125290	—	—	—	—

Table 5
Resume of equations in Appendix B, for the different cases

Case of Fig. 5	II, V, VII	IV, VII		I, III, VI
Optimal sol.	α^*	α^*	α_p	α^*
Equations	(7a), (7b), (7c)	(8a), (8b), (8c)	(9a), (9b), (9c)	(6a), (6b), (6c)
Limit values	$0 < h_f/d \le \frac{17}{66}\left(1+\frac{a}{d}\right)$	$\frac{17}{66}\left(1+\frac{a}{d}\right) < h_f/d \le \alpha^*$	$\frac{17}{66}\left(1+\frac{a}{d}\right) < h_f/d \le \alpha_p$	$h_f/d > \frac{17}{66}\left(1+\frac{a}{d}\right)$

and (8a), given in Appendix B, depending on the depth of neutral axis that changes with the values of h_f/d. The other involved variables, such as a/d; b_w/b and steel class lead to different curves.

Fig. 9(a) is an abacus giving the optimal total area of reinforcement ($A'_s + A_s$) as α function of the applied reduced bending moment μ, and the ratio h_f/d, for $a/d = 0.1$ and $b/b_w = 10$. The distribution of this area of steel between the upper and lower faces, is obtained from Fig. 9(b)). Figs. 10–13, have the same interpretation of Fig. 9, and correspond to the different values of the geometric parameters and a/d=0.1. These figures are resumed in Table 6 and cover some current sections permitting the direct calculation from the figures or employing linear interpolation. Design abacuses for other values of a/d are in [12].

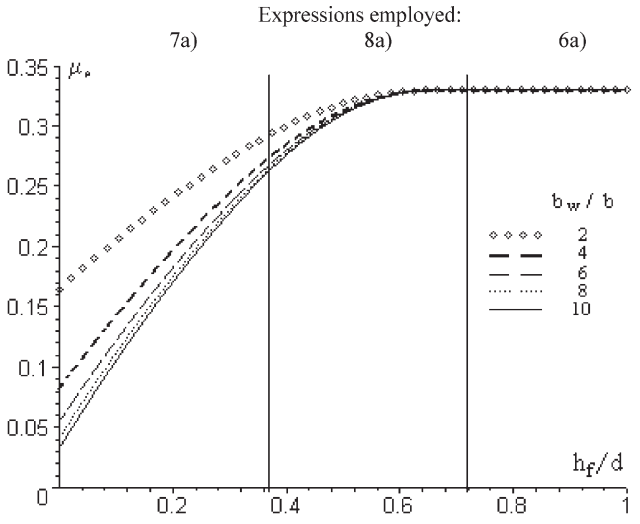

Fig. 8. Economic μ_e for $a/d = 0.1$.

4.2. Numerical results

In this section a comparison is made between the design obtained in the present formulation and the approximated solutions given by CEB [11]. The percentile of total reinforcement, the amount of upper steel area and the errors in percentile are detailed in Table 7.

The percentile of error is calculated by:

$$\text{Error} = \frac{\text{Re } f.[11] - \text{mod } el}{\text{mod } el} \times 100$$

As can be observed in Table 7, the total area of reinforcement has a maximum difference of 2.05% when compared with the CEB solution. Generally the differences in the distribution A'_s/A_s is always larger with a maximum of 10.4%. Although the differences for the required reinforcement do not exceed 10.4% in the studied case, it seems that in repeated structures, such as in prefabrication, this difference can be relevant in econ-

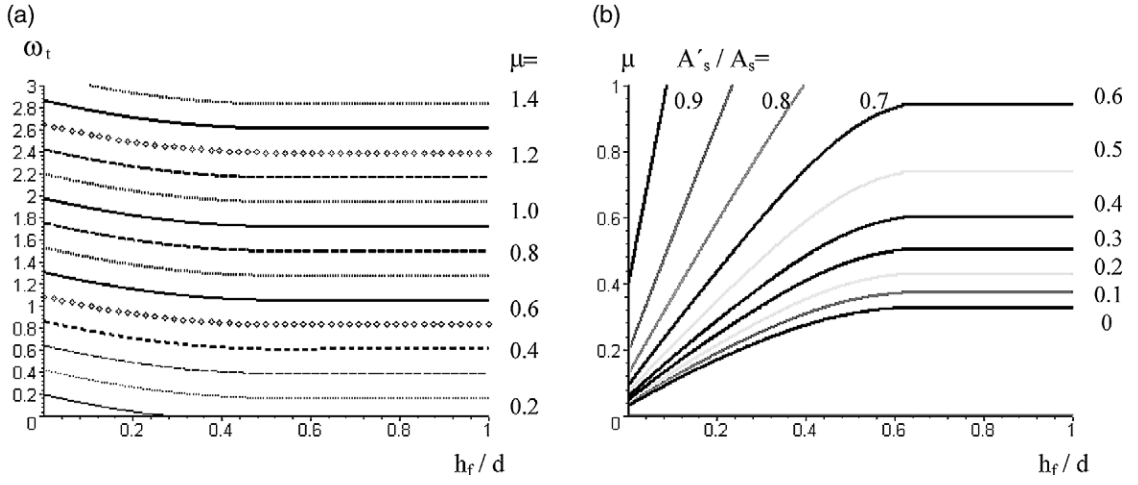

Fig. 9. (a) Increasing in μ with ω_t, for b/b_w=10 (b) μ variation with A'_s/A_s, for b/b_w=10.

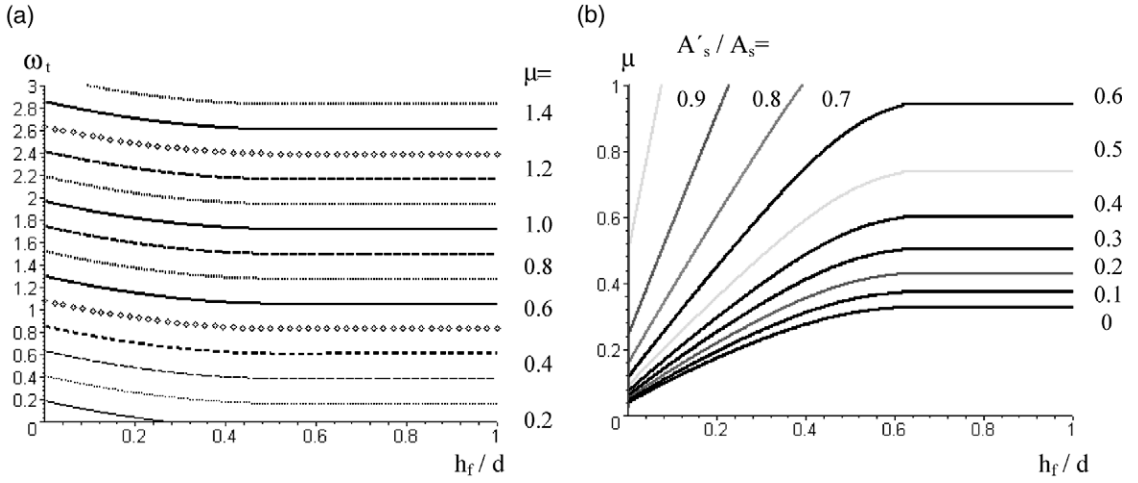

Fig. 10. (a) Increase in μ with ω_t, for $b/b_w = 8$; (b) μ variation with A'_s/A_s, for $b/b_w = 8$.

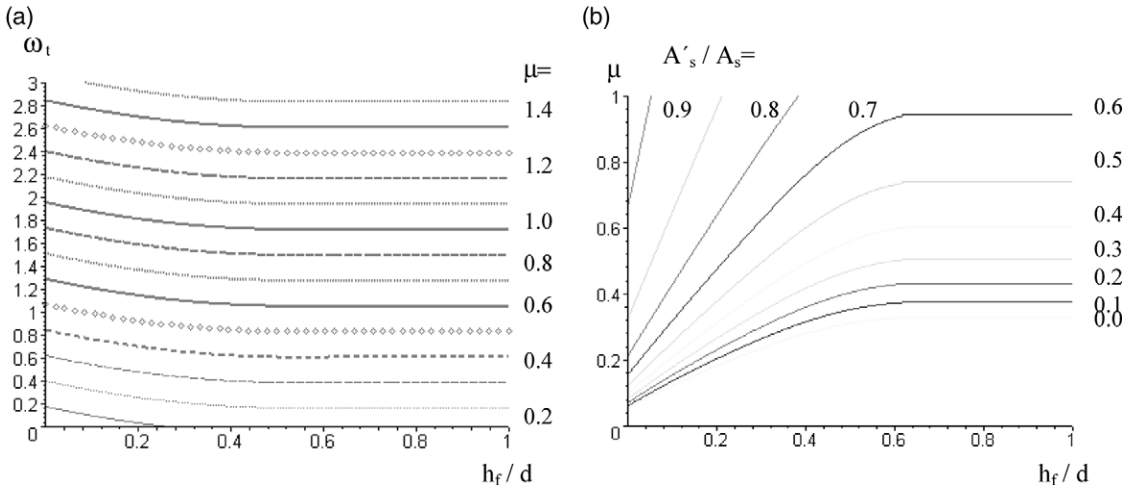

Fig. 11. (a) Increase in μ with ω_t, for $b/b_w = 6$; (b) μ variation with A'_s/A_s, for $b/b_w = 6$.

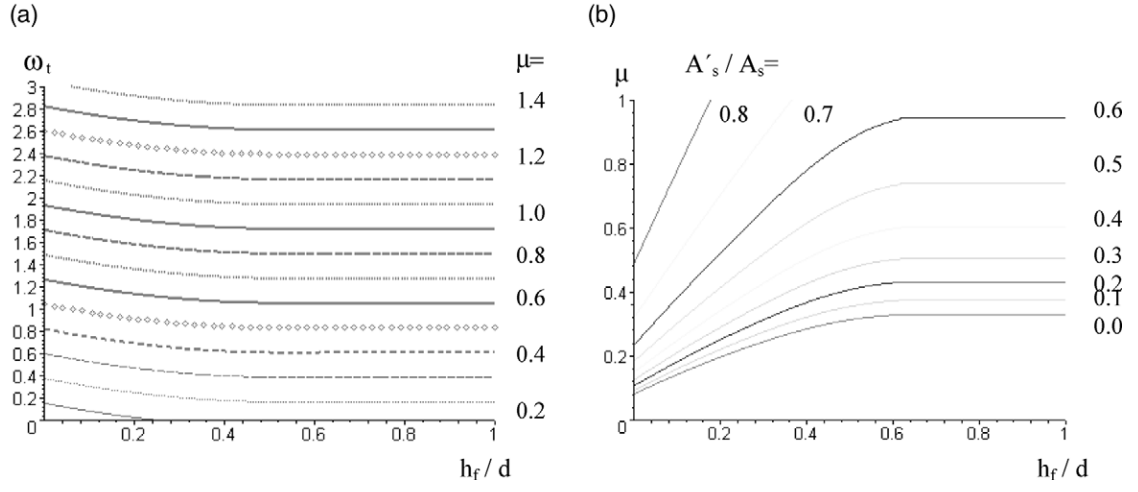

Fig. 12. (a) Increase in μ with ω_t, for $b/b_w = 4$; (b) μ variation with A'_s/A_s, for $b/b_w = 4$.

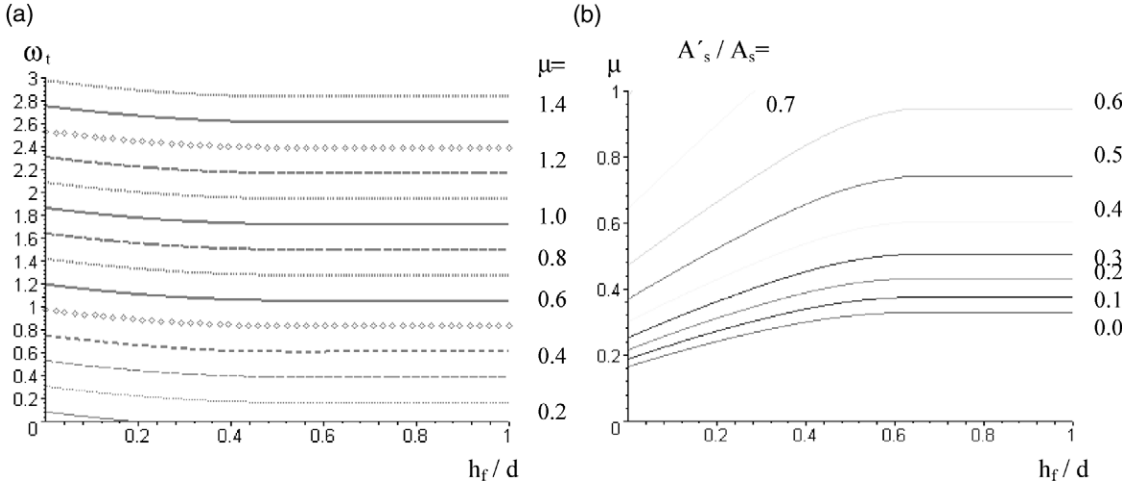

Fig. 13. (a) Increase in μ with ω_t, for $b/b_w = 2$; (b) μ variation with A'_s/A_s, for $b/b_w=2$.

Table 6
Resume of geometric definitions in Figs. 9–13

S400 S500	b/b_w				
	10	8	6	4	2
ω_t	(9a)	(10b)	(11a)	(12a)	(13a)
A'_s/A_s	(9b)	(10b)	(11b)	(12b)	(13b)

omical terms. It can be emphasised that L-, I- and T-sections are commonly used in buildings.

Since the solution obtained in this work is an exact one, it can be noted that the errors in the CEB solution have consequences in terms of: not satisfying the equilibrium Eqs (5) and (8); deviation of the neutral axis and error in the rotation of the section at rupture.

5. Conclusion

In the present work a model is developed for the optimisation of reinforced concrete T-sections, in ultimate design, under bending moment. In the model, the non-linear behaviour of concrete, with parabola–rectangle law for compression and no tensile strength, and elasto-plastic behaviour for steel are considered.

In this work, the equation of maximum value of the bending moment considering only single reinforcement, for T-section is obtained. The equations for the optimal area of reinforcement and corresponding localisation are also presented. These equations are expressed in terms of the geometry and mechanical characteristics as indicated in Appendices A and B. The equations are plotted for current T-section geometric characteristics in Figs. 9–13, for S400 and S500 steel.

The comparison between the results obtained with the optimal design and current practice methods (CEB solution) is made. The advantages of the present model are: the correct solution is economic when compared to current practice solutions; the use of non-linear behaviour of the materials; the development of a methodology that can be extended to other sections; the establishment of the optimal design equations that can be implemented in computer codes.

Acknowledgements

This work was performed under the financial support of the Portuguese Minister of Science and Technology by Programa Operacional do Quadro Comunitário de Apoio (POCTI) and by FEDER grant POCTI/EMC/12126/1998, Fase II.

Appendix A

The resulting reduced compressive force $F^i_{cd_{red}}$ in the concrete and the location X^i of the force F^i_{cd}, indicated in Fig. 4, are listed bellow, for the different cases (see Fig. 5):

$$F^{I}_{cd_{red}} = \frac{17}{12}\frac{\alpha^2}{(\alpha-1)^2}(3-8\alpha);\ X^{I} = \frac{19\alpha-4}{48\alpha-3}\alpha\, d$$

$$F^{II}_{cd_{red}} = \frac{17}{12}\frac{1}{(\alpha-1)^2}\left[\left(21\frac{h_f}{d}\alpha^2-6\frac{h_f}{d}\alpha-18\left(\frac{h_f}{d}\right)^2\alpha+3\left(\frac{h_f}{d}\right)^2+5\frac{b_w}{b}\left(\frac{h_f}{d}\right)^3\right)\left(\frac{b_w}{b}-1\right)-8\frac{b_w}{b}\alpha^3+3\frac{b_w}{b}\alpha^2\right]$$

$$X^{II} = \frac{17d}{48F^{II}_{cd_{red}}(\alpha-1)^2}\left[\left(-42\alpha^2+48\frac{h_f}{d}\alpha+12\alpha-8\frac{h_f}{d}-15\left(\frac{h_f}{d}\right)^2\right)\left(\frac{h_f}{d}\right)^2\left(1-\frac{b_w}{b}\right)+4\frac{b_w}{b}\alpha^3-9\frac{b_w}{b}\alpha^4\right]$$

$$F^{III}_{cd_{red}} = \frac{68}{75}\alpha-\frac{17}{300};\ X^{III} = \frac{d}{20}\frac{1+171\alpha^2-22\alpha}{16\alpha-1}$$

$$F^{IV}_{cd_{red}} = \frac{17}{300(\alpha-1)^2}\left(216\alpha^3+18\alpha-1+\alpha^2\left(75\frac{b_w}{b}-108\right)+\left(\frac{b_w}{b}-1\right)\frac{h_f}{d}(525\alpha^2-150\alpha)+\left(75-450\alpha+125\frac{h_f}{d}\right)\left(\frac{b_w}{b}-1\right)\left(\frac{h_f}{d}\right)^2\right)$$

$$X^{IV} = \frac{17\,d}{F^{IV}_{cd_{red}}6000(\alpha-1)^2}\left((36\alpha^2-12\alpha+1)^2+1875\left(\frac{h_f}{d}\right)^4\left(\frac{b_w}{b}-1\right)+\ +5250\left(\frac{b_w}{b}-1\right)\left(\frac{h_f}{d}\right)^2\alpha^2+\left(\frac{b_w}{b}-1\right)\left(\frac{h_f}{d}\right)^2\left(1000\frac{h_f}{d}(1-6\alpha)-1500\alpha\right)+500\frac{b_w}{b}\alpha^3-1125\frac{b_w}{b}\alpha^4\right)$$

Table 7
Design of a T-section for μ_{sd} = 0.5, 1.0, 2.0 and 3.0

h_f/d		0.05						0.40					
b/b_w		2			10			2			10		
a/d		0.05	0.1	0.15	0.05	0.1	0.15	0.05	0.1	0.15	0.05	0.1	0.15
μ_{sd} =0.5													
ω_t	Model	0.9103	0.9473	0.9881	0.9884	1.0387	1.0948	0.8171	0.8405	0.8661	0.8207	0.8464	0.8752
	Ref. [8]	0.911	0.949	0.991	0.988	1.039	1.095	0.817	0.841	0.869	0.821	0.847	0.877
	%Error	0.07	0.18	0.29	−0.04	0.03	0.02	−0.01	0.06	0.33	0.04	0.07	0.21
$\frac{A_s'}{A_s}$	Model	0.5850	0.5841	0.5846	0.8473	0.8508	0.8546	0.3597	0.3596	0.3608	0.4079	0.4165	0.4266
	Ref.[8]	0.593	0.606	0.619	0.850	0.855	0.862	0.366	0.397	0.393	0.411	0.424	0.438
	%Error	1.37	3.75	5.88	0.32	0.49	0.86	1.75	10.40	8.92	0.76	1.80	2.67
μ_{sd} = 1.0													
	model	1.9629	2.0584	2.1646	2.0410	2.1498	2.2713	1.8697	1.9516	2.0426	1.8733	1.9575	2.0516
	Ref. [8]	1.964	2.060	2.167	2.041	2.150	2.272	1.870	1.952	2.045	1.874	1.959	2.054
	%Error	0.06	0.08	0.11	0.00	0.01	0.03	1.60	2.05	0.12	0.04	0.08	0.12
$\frac{A_s'}{A_s}$	Model	0.7834	0.7844	0.7862	0.9230	0.9250	0.9272	0.6587	0.6627	0.6678	0.6888	0.6976	0.7073
	Ref. [8]	0.787	0.796	0.806	0.924	0.927	0.930	0.668	0.675	0.687	0.690	0.702	0.713
	%Error	0.46	1.48	2.52	0.11	0.22	0.30	1.41	1.86	2.88	0.17	0.63	0.81
μ_{sd} = 2.0													
	Model	4.0682	4.2806	4.5175	4.1463	4.3720	4.6242	3.9750	4.1738	4.3955	3.9786	4.1798	4.4046
	Ref. [8]	4.069	4.282	4.520	4.146	4.372	4.625	3.975	4.175	4.397	3.979	4.181	4.407
	%Error	0.02	0.03	0.06	−0.01	0.00	0.02	0.00	0.03	0.03	0.01	0.03	0.05
$\frac{A_s'}{A_s}$	Model	0.8893	0.8902	0.8915	0.9614	0.9624	0.9636	0.8235	0.8267	0.8306	0.8403	0.8460	0.8521
	Ref. [8]	0.892	0.896	0.902	0.962	0.964	0.966	0.826	0.834	0.841	0.841	0.848	0.856
	%Error	0.30	0.65	1.18	0.06	0.17	0.25	0.30	0.88	1.25	0.08	0.24	0.46
μ_{sd} = 3.0													
	Model	6.1734	6.5029	6.8705	6.2515	6.5942	6.9771	6.0803	6.3961	6.7484	6.0838	6.4020	6.7575
	Ref. [8]	6.175	6.504	6.873	6.252	6.594	6.977	6.080	6.397	6.751	6.084	6.403	6.759
	%Error	0.03	0.02	0.04	0.01	0.00	0.00	0.00	0.01	0.04	0.00	0.02	0.02
$\frac{A_s'}{A_s}$	Model	0.9256	0.9263	0.9273	0.9742	0.9749	0.9557	0.8810	0.8834	0.8863	0.8926	0.8967	0.9010
	Ref.[8]	0.927	0.931	0.934	0.974	0.976	0.977	0.883	0.888	0.894	0.894	0.898	0.903
	%Error	0.15	0.51	0.72	−0.02	0.11	2.23	0.23	0.52	0.87	0.16	0.14	0.22

$$F_{cd_{red}}^{V} = \frac{17h_f}{20d} + \frac{68b_w}{75\,b}\alpha - \frac{17h_f b_w}{20d\,b} - \frac{17\,b_w}{300\,b}$$

$$X^{V} = \frac{d}{20}\frac{150\left(\frac{b_w}{b}-1\right)\left(\frac{h_f}{d}\right)^2 - 171\alpha^2 + 22\alpha - 1}{15\left(\frac{b_w}{b}-1\right)\frac{h_f}{d} - 16\frac{b_w}{b}\alpha + \frac{b_w}{b}}$$

$$F_{cd_{red}}^{VI} = \frac{289}{420}\alpha;\ X_{cd_{red}}^{VI} = \frac{99}{238}\alpha\, d$$

$$F_{cd_{red}}^{VII} = \frac{17}{6720\alpha^2}\left(245\frac{b_w}{b}\alpha^3 - 147\frac{h_f}{d}\alpha^2\left(\frac{b_w}{b}-1\right) - 441\left(\frac{h_f}{d}\right)^2\alpha\left(\frac{b_w}{b}-1\right) + 343\left(\frac{h_f}{d}\right)^3\left(\frac{b_w}{b}-1\right) + 27\alpha^3\right)$$

$$\bar{X}^{VIII} = \frac{3d}{28}\frac{1029\frac{b_w}{b}\alpha^4 - 686\left(\frac{h_f}{d}\right)^2\alpha^2\left(\frac{b_w}{b}-1\right) - 2744\left(\frac{h_f}{d}\right)^3\alpha\left(\frac{b_w}{b}-1\right) + 2401\left(\frac{h_f}{d}\right)^4\left(\frac{b_w}{b}-1\right) + 27\alpha^4}{245\frac{b_w}{b}\alpha^3 - 147\frac{h_f}{d}\alpha^2\left(\frac{b_w}{b}-1\right) - 441\left(\frac{h_f}{d}\right)^2\alpha\left(\frac{b_w}{b}-1\right) + 343\left(\frac{h_f}{d}\right)^3\left(\frac{b_w}{b}-1\right) + 27\alpha^3}$$

$$F_{cd_{red}}^{VIII} = \frac{17h_f}{20d} + \frac{289b_w}{420\,b}\alpha - \frac{17h_f b_w}{20d\,b}$$

$$X^{VIII} = \frac{3d}{14}\frac{-49\left(\frac{h_f}{d}\right)^2 + 49\frac{b_w}{b}\left(\frac{h_f}{d}\right)^2 - 33\frac{b_w}{b}\alpha^2}{-21\frac{h_f}{d} - 17\frac{b_w}{b}\alpha + 21\frac{b_w h_f}{b\,d}}$$

Appendix B

The optimal design of the sections referred to in section 3.5, with the limits referred in Table 5, can be represented by the following expressions:

$$\mu_e \geq \frac{4913}{47520}\left(1+\frac{a}{d}\right)\left(3-\frac{a}{d}\right). \tag{6a}$$

$$\left(\frac{A_s'}{A_s}\right)^* = \frac{14739 + 9826\frac{a}{d} - 4913\left(\frac{a}{d}\right)^2 - 47520\mu}{-4913 + 9826\frac{a}{d} + 14739\left(\frac{a}{d}\right)^2 - 47520\mu}, \tag{6b}$$

$$w^* = \frac{-4913 + 9826\frac{a}{d} + 14739\left(\frac{a}{d}\right)^2 - 47520\mu}{47520\left(\frac{a}{d}-1\right)} \tag{6c}$$

$$\mu_e \geq \frac{17h_f}{20d}\left(1-\frac{b_w}{b}\right) + \frac{4913\,b_w}{15840\,b} + \frac{4913\,b_w a}{23760\,b\,d} - \frac{17}{40}\left(\frac{h_f}{d}\right)^2\left(1-\frac{b_w}{b}\right) - \frac{4913\,b_w}{47520\,b}\left(\frac{a}{d}\right)^2 \tag{7a}$$

$$\left(\frac{A_s'}{A_s}\right)^* = \frac{40392\frac{h_f}{d}\left(1-\frac{b_w}{b}\right) - 20196\left(\frac{h_f}{d}\right)^2\left(1-\frac{b_w}{b}\right) + 14739\frac{b_w}{b} + 9826\frac{b_w a}{b\,d} - 4913\frac{b_w}{b}\left(\frac{a}{d}\right)^2 - 47520\mu}{-20196\left(\frac{h_f}{d}\right)^2\left(1-\frac{b_w}{b}\right) - 4913\frac{b_w}{b} + 9826\frac{b_w a}{b\,d} + 14739\frac{b_w}{b}\left(\frac{a}{d}\right)^2 + 40392\frac{h_f a}{d\,d}\left(1-\frac{b_w}{b}\right) - 47520\mu} \tag{7b}$$

$$\omega^* = \frac{1}{47520\left(\frac{a}{d}-1\right)}\left[\left(40392\frac{h_f a}{d\,d} - 20196\left(\frac{h_f}{d}\right)^2\right)\left(1-\frac{b_w}{b}\right) - 4913\frac{b_w}{b}\left(1-2\frac{a}{d}\right) + 14739\frac{b_w}{b}\left(\frac{a}{d}\right)^2 - 47520\mu\right] \tag{7c}$$

$$\mu_e \geq \frac{-1}{284359680\left(1+\frac{a}{d}\right)^2}\left[-105746256\frac{h_f}{d}\left[1-\frac{b_w}{b} - \frac{b_w}{b}\left(\frac{a}{d}\right)^2 + \left(\frac{a}{d}\right)^2\right] - 77276577\frac{b_w}{b} - 32013108\frac{a}{d} + + (351895104\frac{a}{d} + 1034985600)\left(\frac{h_f}{d}\right)^3\left(1-\frac{b_w}{b}\right) - 512317872\left(\frac{h_f}{d}\right)^4\left(1-\frac{b_w}{b}\right) + 751689\left(\frac{a}{d}\right)^4 - -10921599 - 422096400\left(\frac{h_f}{d}\right)^2\frac{a}{d}\left(1-\frac{b_w}{b}\right) + 52873128\left(\frac{h_f}{d}\right)^2\left(\frac{a}{d}\right)^2\left(1-\frac{b_w}{b}\right) - 30509730\left(\frac{a}{d}\right)^2 + 211492512\frac{h_f a}{d\,d}\left(1-\frac{b_w}{b}\right) - 474969528\left(\frac{h_f}{d}\right)^2\left(1-\frac{b_w}{b}\right) + 28647703\left(\frac{a}{d}\right)^4\frac{b_w}{b} - 145886622\left(\frac{a}{d}\right)^2\frac{b_w}{b} - - 203182028\frac{b_w a}{b\,d} + 8666532\left(\frac{a}{d}\right)^3\left(\frac{b_w}{b}-1\right)\right] \tag{8a}$$

$$(A'_s/A_s)^* = K_A/K_B, \text{ with } K_A = 8666532\frac{a}{d}\left(\frac{b_w}{b}-1\right) + 284359680\mu\left[1+\left(\frac{a}{d}\right)^2\right] - 105746256\frac{a h_f}{d\,d}\left[1+\left(\frac{a}{d}\right)^2 - \frac{b_w}{b} - \frac{b_w}{b}\left(\frac{a}{d}\right)^2\right] + + \left[422096400\frac{a}{d} - 52873128 - 1034985600\frac{a h_f}{d\,d} - 351895104\frac{h_f}{d}\right.$$

$$+ 512317872\left(\frac{h_f}{d}\right)^2 + 474969528\left(\frac{a}{d}\right)^2\Big].\left(\frac{h_f}{d}\right)^2\left(\frac{b_w}{b} - 1\right) + 28647703\frac{b_w}{b} - 10921599\left(\frac{a}{d}\right)^4 + 751689 + \left[211492512\left(\frac{b_w}{b} - 1\right)\frac{h_f}{d} - 30509730\right]\left(\frac{a}{d}\right)^2 + + 568719360\,\mu\frac{a}{d} - 203182028\frac{b_w}{b}\left(\frac{a}{d}\right)^3 - 77276577\frac{b_w}{b}\left(\frac{a}{d}\right)^4 - 145886622\frac{b_w}{b}\left(\frac{a}{d}\right)^2 - 32013108\left(\frac{a}{d}\right)^3, \quad (8b)$$

$$K_B = -52873128\left(\frac{b_w}{b} - 1\right)\frac{h_f}{d}\left[\left(\frac{a}{d}\right)^2\left(\frac{h_f}{d} + 2\right) - 2\right] + 284359680\mu\left[1 + \left(\frac{a}{d}\right)^2\right] - 32013108\frac{a}{d}77276577\frac{b_w}{b} + + 216\left(\frac{b_w}{b} - 1\right)\frac{h_f}{d}\left[1954150\frac{ah_f}{dd} + 2198933\frac{h_f}{d} + 979132\frac{a}{d} + 2371842\left(\frac{h_f}{d}\right)^3\right] - 203182028\frac{b_w a}{b\,d} - -15552\left(\frac{b_w}{b} - 1\right)\left(\frac{h_f}{d}\right)^3\left(226227\frac{a}{d} + 66550\right) + 8666532\left(\frac{b_w}{b} - 1\right)\left(\frac{a}{d}\right)^3 + 28647703\frac{b_w}{b}\left(\frac{a}{d}\right)^4 - 10921599 + + 751689\left(\frac{a}{d}\right)^4 - 30509730\left(\frac{a}{d}\right)^2 - 145886622\frac{b_w}{b}\left(\frac{a}{d}\right)^2 + 568719360\frac{a}{d}\mu$$

$$\omega^* = \frac{-1}{284359680\left(1 + \frac{a}{d}\right)^2\left(\frac{a}{d} - 1\right)}\Bigg[\Bigg(1034985600\frac{a}{d} + 351895104\Bigg)\left(\frac{h_f}{d}\right)^3\left(1 - \frac{b_w}{b}\right) - 8666532\frac{a}{d}\left(1 - \frac{b_w}{b}\right) + 28647703\frac{b_w}{b} + 284359680\,\mu\left(1 + \left(\frac{a}{d}\right)^2\right) - 512317872\left(\frac{h_f}{d}\right)^4\left(1 - \frac{b_w}{b}\right) - 10921599\left(\frac{a}{d}\right)^4 + 751689 - 422096400\left(\frac{h_f}{d}\right)^2\frac{a}{d}\left(1 - \frac{b_w}{b}\right) + (52873128 - 474969528\left(\frac{a}{d}\right)^2)\left(\frac{h_f}{d}\right)^2\left(1 - \frac{b_w}{b}\right) - 32013108\left(\frac{a}{d}\right)^3 - -105746256\left(\frac{a}{d}\right)^3\frac{h_f}{d}\left(1 - \frac{b_w}{b}\right) - 211492512\left(\frac{a}{d}\right)^2\frac{h_f}{d}\left(1 - \frac{b_w}{b}\right) - 30509730\left(\frac{a}{d}\right)^2 + 568719360\mu\frac{a}{d} - - 105746256\frac{h_f a}{d\,d}\left(1 - \frac{b_w}{b}\right) - 203182028\left(\frac{a}{d}\right)^3\frac{b_w}{b} - 77276577\frac{b_w}{b}\left(\frac{a}{d}\right)^4 - 145886622\frac{b_w}{b}\left(\frac{a}{d}\right)^2\Bigg] \quad (8c)$$

$$\mu_e \geq -\frac{17}{3840(7 + 2000\varepsilon_{syd})^2}\Bigg[-3773\frac{b_w}{b} - 216000\varepsilon_{syd} - 675 - 196 \times 10^4\frac{b_w}{b}\varepsilon_{syd} + \left(\frac{b_w}{b} - 1\right)\Bigg[4116\frac{h_f}{d} + + 7203\left(\frac{h_f}{d}\right)^4 - 17836\left(\frac{h_f}{d}\right)^3 - 1088 \times 10^9\left(\frac{h_f}{d}\right)^3\varepsilon_{syd}^3 - 672 \times 10^7\left(\frac{h_f}{d}\right)^3\varepsilon_{syd}^2 + 2856 \times 10^6\left(\frac{h_f}{d}\right)^2\varepsilon_{syd}^2 - 64 \times 10^{12}\left(\frac{h_f}{d}\right)^3\varepsilon_{syd}^4 + 48 \times 10^{12}\left(\frac{h_f}{d}\right)^4\varepsilon_{syd}^4 + 336 \times 10^6\left(\frac{h_f}{d}\right)\varepsilon_{syd}^2 + 8232 \times 10^3\left(\frac{h_f}{d}\right)^4\varepsilon_{syd} + 10290\left(\frac{h_f}{d}\right)^2 - 18032 \times 10^3\left(\frac{h_f}{d}\right)^3\varepsilon_{syd} + 9408 \times 10^3\left(\frac{h_f}{d}\right)^2\varepsilon_{syd} + 2352 \times 10^3\left(\frac{h_f}{d}\right)\varepsilon_{syd} + 672 \times 10^9\left(\frac{h_f}{d}\right)^4\varepsilon_{syd}^3 + 288 \times 10^9\left(\frac{h_f}{d}\right)^2\varepsilon_{syd}^3 + 3528 \times 10^6\left(\frac{h_f}{d}\right)^4\varepsilon_{syd}^2\Bigg] \quad (9a)$$

$$\left(\frac{A_s}{A_c}\right)^* = \frac{69972\frac{h_f}{d}\left(\frac{b_w}{b} - 1\right) - 64141\frac{b_w}{b} + 188160\mu + 303212\left(\frac{h_f}{d}\right)^3\left(1 - \frac{b_w}{b}\right) - 122451\left(\frac{h_f}{d}\right)^4\left(1 - \frac{b_w}{b}\right)}{52479\frac{b_w}{b} + 188160\mu + 139944\left(\frac{h_f}{d}\right)^3\left(1 - \frac{b_w}{b}\right) - 122451\left(\frac{h_f}{d}\right)^4\left(1 - \frac{b_w}{b}\right) + 1377} \quad (9b)$$

$$\times \frac{-11475 - 3672000\varepsilon_{syd} - 18496 \times 10^9\left(\frac{h_f}{d}\right)^3\left(\frac{b_w}{b} - 1\right)\varepsilon_{syd}^3 - 306544000\left(\frac{h_f}{d}\right)^3\left(\frac{b_w}{b} - 1\right)\varepsilon_{syd}}{-3264 \times 10^9\left(\frac{h_f}{d}\right)^3\left(\frac{b_w}{b} - 1\right)\varepsilon_{syd}^3 - 119952000\left(\frac{h_f}{d}\right)^3\left(\frac{b_w}{b} - 1\right)\varepsilon_{syd} - 34272 \times 10^6\left(\frac{h_f}{d}\right)^3\left(\frac{b_w}{b} - 1\right)\varepsilon_{syd}^2}$$

$$\frac{-11424 \times 10^7\left(\frac{h_f}{d}\right)^3\left(\frac{b_w}{b} - 1\right)\varepsilon_{syd}^2 + 159936000\left(\frac{h_f}{d}\right)^2\left(\frac{b_w}{b} - 1\right)\varepsilon_{syd} + 48552 \times 10^6\left(\frac{h_f}{d}\right)^2\left(\frac{b_w}{b} - 1\right)\varepsilon_{syd}^2 + 39984000\frac{h_f}{d}\left(\frac{b_w}{b} - 1\right)\varepsilon_{syd}}{-19992000\left(\frac{h_f}{d}\right)^2\left(\frac{b_w}{b} - 1\right)\varepsilon_{syd} - 2856 * 10^6\left(\frac{h_f}{d}\right)^2\left(\frac{b_w}{b} - 1\right)\varepsilon_{syd}^2 + 11424 \times 10^9\left(\frac{h_f}{d}\right)^4\left(\frac{b_w}{b} - 1\right)^3_{sydc} + 81610^{12}\left(\frac{h_f}{d}\right)^4\left(\frac{b_w}{b} - 1\right)\varepsilon_{syd}^4}$$

$$\times \frac{-1088 \times 10^{12}\left(\frac{h_f}{d}\right)^3\left(\frac{b_w}{b}-1\right)\varepsilon_{syd}^4 + \left(\frac{h_f}{d}\right)^4\left(\frac{b_w}{b}-1\right)(11424 \times 10^9\varepsilon_{syd}^3 + 816 \times 10^{12}\varepsilon_{syd}^4) + 4896 \times 10^9\left(\frac{h_f}{d}\right)^2\left(\frac{b_w}{b}-1\right)\varepsilon_{syd}^3}{\left(\frac{h_f}{d}\right)^4\left(\frac{b_w}{b}-1\right)(59976 \times 10^6\varepsilon_{syd}^2 + 139944000\varepsilon_{syd}) - 34986\left(\frac{h_f}{d}\right)^2\left(\frac{b_w}{b}-1\right) + 1536 \times 10^7\varepsilon_{syd}^2\mu + 10752000\varepsilon_{syd}\mu}$$

$$\frac{5712x10^6\left(\frac{h_f}{d}\right)\left(\frac{b_w}{b}-1\right)\varepsilon_{syd}^2 + 59976 \times 10^6\left(\frac{h_f}{d}\right)^4\left(\frac{b_w}{b}-1\right)\varepsilon_{syd}^2 + 139944000\left(\frac{h_f}{d}\right)^4\left(\frac{b_w}{b}-1\right)\varepsilon_{syd} + 1536 \times 10^7\varepsilon_{syd}^2\mu}{-12852\frac{a}{d} + \frac{a}{d}\left(\frac{h_f}{d}\right)^3\left(\frac{b_w}{b}-1\right)(-163268 - 15232 \times 10^9\varepsilon_{syd}^3 - 79968 \times 10^6\varepsilon_{syd}^2 - 1088 \times 10^{12} \times 10^6\varepsilon_{syd}^4 - 186592000\varepsilon_{syd})}$$

$$\frac{174930\left(\frac{h_f}{d}\right)^2\left(\frac{b_w}{b}-1\right) - 33320000\left(\frac{b_w}{b}\right)\varepsilon_{syd} + 107520000\varepsilon_{syd}\mu}{+\frac{a}{d}\left(\frac{h_f}{d}\right)^2\left(\frac{b_w}{b}-1\right)(+51408 \times 10^6\varepsilon_{syd}^2 + 4896 \times 10^9\varepsilon_{syd}^3 + 179928000\varepsilon_{syd} + 209916) - 3672000\frac{a}{d}\varepsilon_{syd} - 33320000\frac{a}{d}\left(\frac{b_w}{b}\right)\varepsilon_{syd}}$$

$$\times \frac{1}{+5712 \times 10^6\frac{a}{d}\left(\frac{h_f}{d}\right)\left(\frac{b_w}{b}-1\right)\varepsilon_{syd}^2 - 116620\frac{b_w a}{b d} + \frac{a}{d}\left(\frac{h_f}{d}\right)\left(\frac{b_w}{b}-1\right)(39984000\varepsilon_{syd} + 69972)}$$

$$\omega^* = -\frac{1}{3840(2000\varepsilon_{syd} + 7)\left(1-\frac{a}{d}\right)(2000\varepsilon_{syd}-7)}\Bigg[52479\frac{b_w}{b} + 188160\mu$$

$$+ 139944\left(\frac{h_f}{d}\right)^3\left(1-\frac{b_w}{b}\right) + \left(1-\frac{b_w}{b}\right)\left(-122451\left(\frac{h_f}{d}\right)^4 + 34986\left(\frac{h_f}{d}\right)^2 + 3264\right.$$

$$\times 10^9\left(\frac{h_f}{d}\right)^3\varepsilon_{syd}^3 - 59976 \times 10^6\left(\frac{h_f}{d}\right)^4\varepsilon_{syd}^2\Bigg) + 1377 + \left(1-\frac{b_w}{b}\right)\left(\frac{h_f}{d}\right)^3(34272$$

$$\times 10^6\varepsilon_{syd}^2 + 119952000\varepsilon_{syd}) + \left(1-\frac{b_w}{b}\right)\left(\frac{h_f}{d}\right)^2(2856 \times 10^6\varepsilon_{syd}^2$$

$$+ 119992000\varepsilon_{syd}) + \left(1-\frac{b_w}{b}\right)\left(\frac{h_f}{d}\right)^4(-816x10^{12}\varepsilon_{syd}^4 - 139944000\varepsilon_{syd} - 11424$$

$$\times 10^9\varepsilon_{syd}^3) - 12852\frac{a}{d} + 163268\frac{a}{d}\left(\frac{h_f}{d}\right)^3\left(1-\frac{b_w}{b}\right) - 1088 \times 10^{12}\frac{a}{d}\left(\frac{h_f}{d}\right)^3\varepsilon_{syd}^4\left(\frac{b_w}{b}\right.$$

$$\left.-1\right) + 39984000\frac{a}{d}\left(\frac{h_f}{d}\right)\varepsilon_{syd}\left(\frac{b_w}{b}-1\right) + 186592000\frac{a}{d}\left(\frac{h_f}{d}\right)^3\varepsilon_{syd}\left(1-\frac{b_w}{b}\right) \qquad (9c)$$

$$+ 5712 \times 10^6\frac{h_f a}{d d}\varepsilon_{syd}^2\left(\frac{b_w}{b}-1\right) + 4896 \times 10^9\frac{a}{d}\left(\frac{b_w}{b}-1\right)\varepsilon_{syd}^3\left(\frac{h_f}{d}\right)^2 - 15232$$

$$\times 10^9\frac{a}{d}\left(\frac{b_w}{b}-1\right)\varepsilon_{syd}^3\left(\frac{h_f}{d}\right)^3 + 79968 \times 10^6\frac{a}{d}\left(\frac{h_f}{d}\right)^3\varepsilon_{syd}^2\left(1-\frac{b_w}{b}\right)$$

$$-33320000\frac{a}{d}\varepsilon_{syd}\frac{b_w}{b} + 179928000\frac{a}{d}\left(\frac{b_w}{b}-1\right)\varepsilon_{syd}\left(\frac{h_f}{d}\right)^2 - 3672000\frac{a}{d}\varepsilon_{syd}$$

$$-51408 \times 10^6\frac{a}{d}\left(\frac{h_f}{d}\right)^2\varepsilon_{syd}^2 + 209916\frac{a}{d}\left(\frac{b_w}{b}-1\right)\left(\frac{h_f}{d}\right)^2 + 69972\frac{a h_f}{d d}\left(\frac{b_w}{b}-1\right)$$

$$-116620\frac{a b_w}{d b} + 51408 \times 10^6\frac{a}{d}\left(\frac{b_w}{b}\right)\left(\frac{h_f}{d}\right)^2\varepsilon_{syd}^2 + 1536 \times 10^7\varepsilon_{syd}^3\mu$$

$$+ 107520000\varepsilon_{syd}\mu]$$

References

[1] Yen JYR. Optimized direct design of reinforced concrete columns with uniaxial loads. ACI Structural Journal 1990;May-June:247–51.

[2] Kangasundram S, Karihaloo BL. Minimum cost design of reinforced concrete structures. Structural Optimization 1990;2:173–84.

[3] Adamu A, Karihaloo BL. Minimum cost reinforced concrete beams using continuum-type optimality criteria structures. Structural Optimization 1994;7:91–102.

[4] Adamu A, Karihaloo BL. Minimum cost design of R.C. T-beams using DCOC. 2nd International Conference on Computational Structures Technology, Athens, Greece, 1994;151–160.

[5] Al-Salloum YA, Siddiqi GH. Cost-optimum minimum design of reinforced concrete beams. ACI Structural Journal 1994;Nov-Dec:647–55.

[6] Eurocode 2, Design of concrete structures, CEN; 1991.

[7] American Concrete Institute, Building code requirements for structural concrete, ACI 318-95, Detroit; 1995.

[8] Rodriguez JA, Ochoa JDA. Biaxial interaction diagrams for short RC columns of any cross section. Journal Structural Engineering ASCE 1999;125(6):672–83.

[9] Fafitis A. Interaction surfaces for of reinforced concrete sections in biaxial bending. Journal Structural Engineering ASCE 2001;127(7):840–6.

[10] Bonet JL, Miguel PF, Romero ML, Fernandez MAA. A modified algorithm for reinforced concrete cross sections integration. In: Proceedings of VI Int. Conf. Computational Structures Technology. Scotland: Civil-Comp Press; 2002.

[11] CEB/FIP, Manual on bending and compression, Committee Euro-International du Beton Construction Press, bulletin no.141; 1982.

[12] Ferreira CC, Melão Barros MHF, Barros AFM. Optimização da Armadura de Secções de Betão Armado em T sob Flexão Simples, VII Congresso de Mecânica Aplicada e Computacional, Abril 2003, Univ. Évora, Portugal.